# Supporting Information

## Fabrication of High-performance Facilitated Transport Membranes for CO$_2$ Separation

**Jiayou Liao, Zhi Wang\*, Chengyun Gao, Shichun Li, Zhihua Qiao, Ming Wang, Song Zhao, Xianmei Xie, Jixiao Wang, and Shichang Wang**

## 1 Thermogravimetry-mass spectrometry (TG-MS) and N$_2$ adsorption-desorption Characterization of hydrotalcite (HT) and layerd double oxide(LDO)
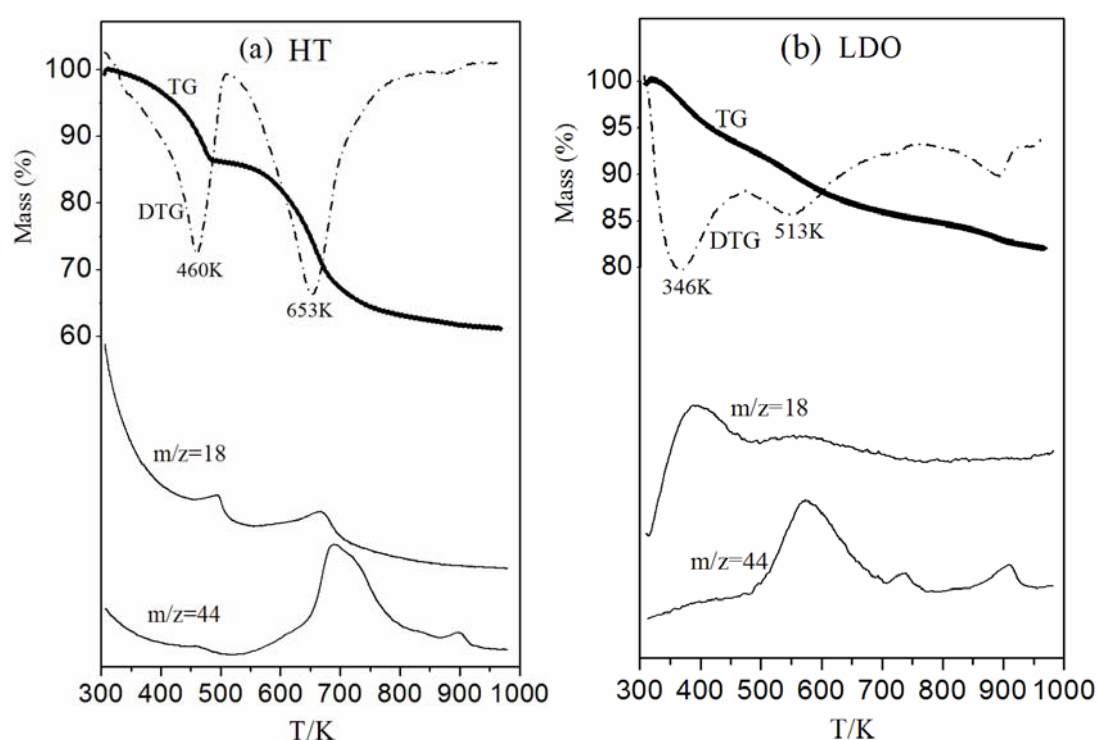


**Figure S1.** TG-MS spectra of (a) HT; (b) LDO.

Figure S1(a) presents the TG-MS diagrams for HT. The TG profile indicates two major weight losses. The first at about 460K ascribes to interlayer water loss (m/z=18); the second at about 653K corresponds to the loss of water from the decomposition of OH groups in the host layers and the removing CO$_2$ from decomposition of interlayer carbonate anions (m/z=44)[1-3]. At the same time, the TG profile also shows a small weight loss below 400K, which attributes to adsorption of water in the environment for the sample. In the TG-MS curves of LDO (Figure S1 (b)), gradual weight loss is also observed with increasing temperature. The weight loss around 346K is assigned to the loss of water, which was adsorbed by LDO from the environment. It is worthwhile to note that an amount of CO$_2$ was released around 513K. The reason is that the LDO was obtained from calcined HT in the air without any protective gas, which leads

to the adsorption of $CO_2$ from the environment for LDO. And the adsorption of $CO_2$ creates necessary conditions for LDO to reconstruct HT in PEIE solution. Concurrently, the $N_2$ adsorption-desorption analysis shows that LDO has larger BET surface area and pore volume than HT (Table S1), which means that LDO is more loose and porous.

**Table S1**. BET surface area and porosity characteristics of HT and LDO obtained from $N_2$ adsorption-desorption data

| sample | BET surface area ($m^2g^{-1}$) | Pore volume ($cm^3g^{-1}$) |
|--------|-------------------------------|---------------------------|
| HT | 82.8040 | 0.6725 |
| LDO | 247.5685 | 0.9092 |

## 2 Chemical structure analysis of PEIE-HT Complex

## (1) ATR-FTIR analysis

The ATR- FTIR spectra of the hydrotalcite(HT) is shown in Figure S2(a). An intense and broad peak at $3426cm^{-1}$ is ascribed to the stretching vibration of hydroxyl groups of HT host layer layers and interlayer water molecules[4-6]. A band is also observed at $1366cm^{-1}$ and this feature has been attributed to the vibrational absorption of interlayer $CO_3^{2-}$ [7]. At the same time, the absorption bands around 600-$900cm^{-1}$ is assigned to M-O (M=Mg, Al)[8]. The result shows that the sample has the typical brucite-like layer of hydrotalcite and the presence of mobile anions and water in the interlayer. The ATR-FTIR spectrum of the PEIE is shown in Figure S2 (b). The broad absorption bands around $3268cm^{-1}$ and $3426cm^{-1}$ are assigned to amino-group and hydroxyl, respectively[9-11], whereas the presence of the alkyl stretch at $2922cm^{-1}$ and $2843cm^{-1}$ indicates that the alkyl chain are attached to the amino-group and hydroxyl[12, 13]. The absorption bands of the N-H and C-H are 1555 $cm^{-1}$ and 1461 $cm^{-1}$ respectively[14]. The peaks at $1406cm^{-1}$, $1296cm^{-1}$are assigned to the OH deformation vibration, while the peaks at $1100cm^{-1}$, $1050cm^{-1}$ are attributed to the stretching of C-O[10, 15, 16]. The result indicates that the polymer has a derivative structure of polyethyleinimine (PEI) and contains a certain amount of hydroxyl group. The Figure S2 (c) is the ATR-FTIR spectrum of PEIE-HT complex. It shows that the characteristics absorption peak of HT was observed in PEIE-HT complex: the interlayer carbonate ions ($CO_3^{2-}$) characteristic absorption peak at $1366cm^{-1}$, the stretching vibrations peak of OH on host layer around $3426cm^{-1}$ and the absorption bands of M-OH(M=Mg, Al) around 600-$900cm^{-1}$, which indicate that the HT reconstructed in PEIE solution successfully. Moreover, the absorption bands of the PEIE were appeared in PEIE-HT complex too. But the absorption bands at $1406cm^{-1}$ and $1296cm^{-1}$, which are assigned to the deformation vibration of OH on the PEIE alkyl stretch, become weak, because the hydroxyl groups of the PEIE were consumed partly with the occurrence of the coupling reaction. Besides, the a new peak at $1265cm^{-1}$ is attributed to the stretching of Si-C[17-20]. The absorption bands around $1100cm^{-1}$ are assigned to the C-O-Si and C-O stretching vibrations, and the absorption bands around

1050cm$^{-1}$ are assigned to the Si-O-M(Mg, Al) [20-22] and C-O. The results showed that the PEIE and HT were coupled successfully by using the APTES as the molecular bridge.
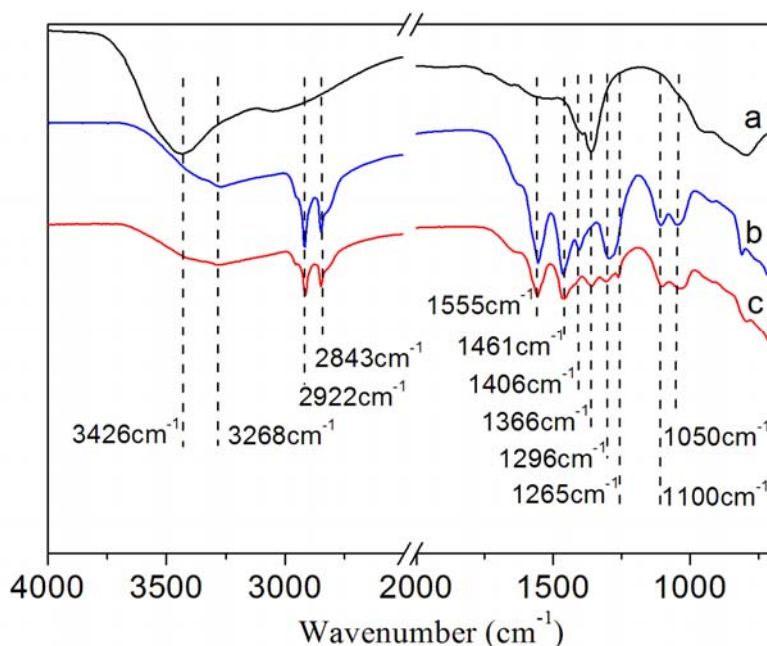


**Figure S2.** ATR-FTIR spectra of (a) HT; (b) PEIE; (c) PEIE-HT complex.

## (2) XPS analysis

As illustrated in Figure S3, C1s spectra of the PEIE-HT complex show peaks at 282.8, 284.6, 285.7, 286.5 and 288.3eV which correspond to C-Si ,C-C/C-H, C-N, C-O-Si/ C-O-H and $CO_3^{2-}$, respectively[23-30]. The Si2p orbital consists of Si- C, Si-O-Mg, and Si-O-C groups that occur at normalized binding energies of 100.8eV, 101.6eV, and 102.5eV, respectively[24, 31-36]. Figure S3(c) shows that Mg2p spectra have peaks at 49.3 eV and 48.4 eV which correspond to Mg-O-H group and Mg-O-Si group, respectively[29, 37, 38]. In Figure S3(d), the narrow scan of Al2p region shows a peak at 73.8eV corresponding to Al-O-H of LDHs group and a peak at 73.1 eV corresponding to Al-O-Si group[38-40]. The XPS analysis indicate that the PEIE-HT complex contains both C-O-Si groups and M (Mg,Al)-O-Si groups. The results show that the silane coupling agent (APTES) played the role of the molecular bridge between the PEIE and the HT through reacting with the hydroxyl groups on the polymers and HT host layers.
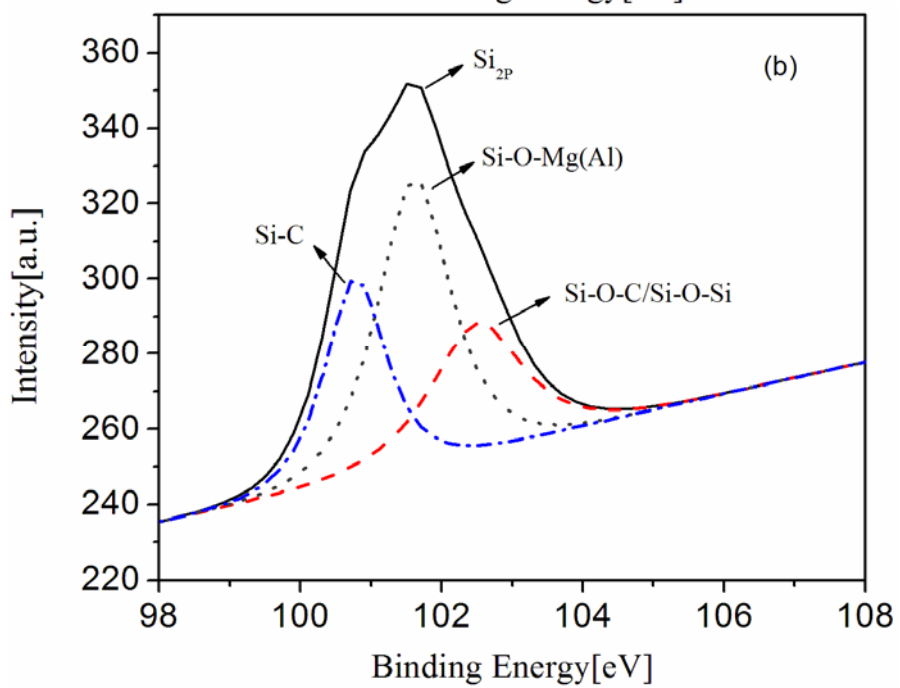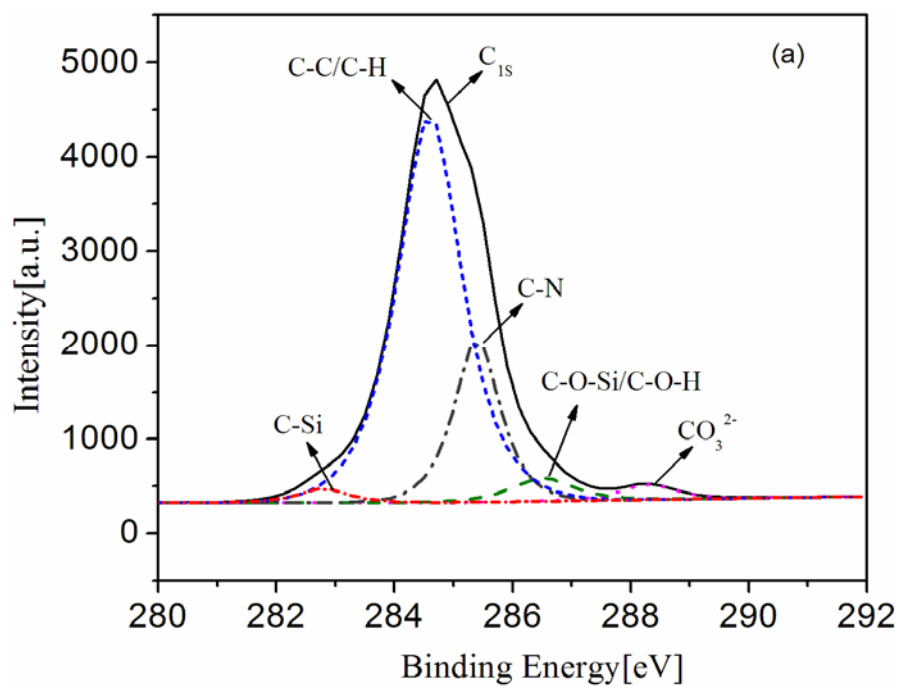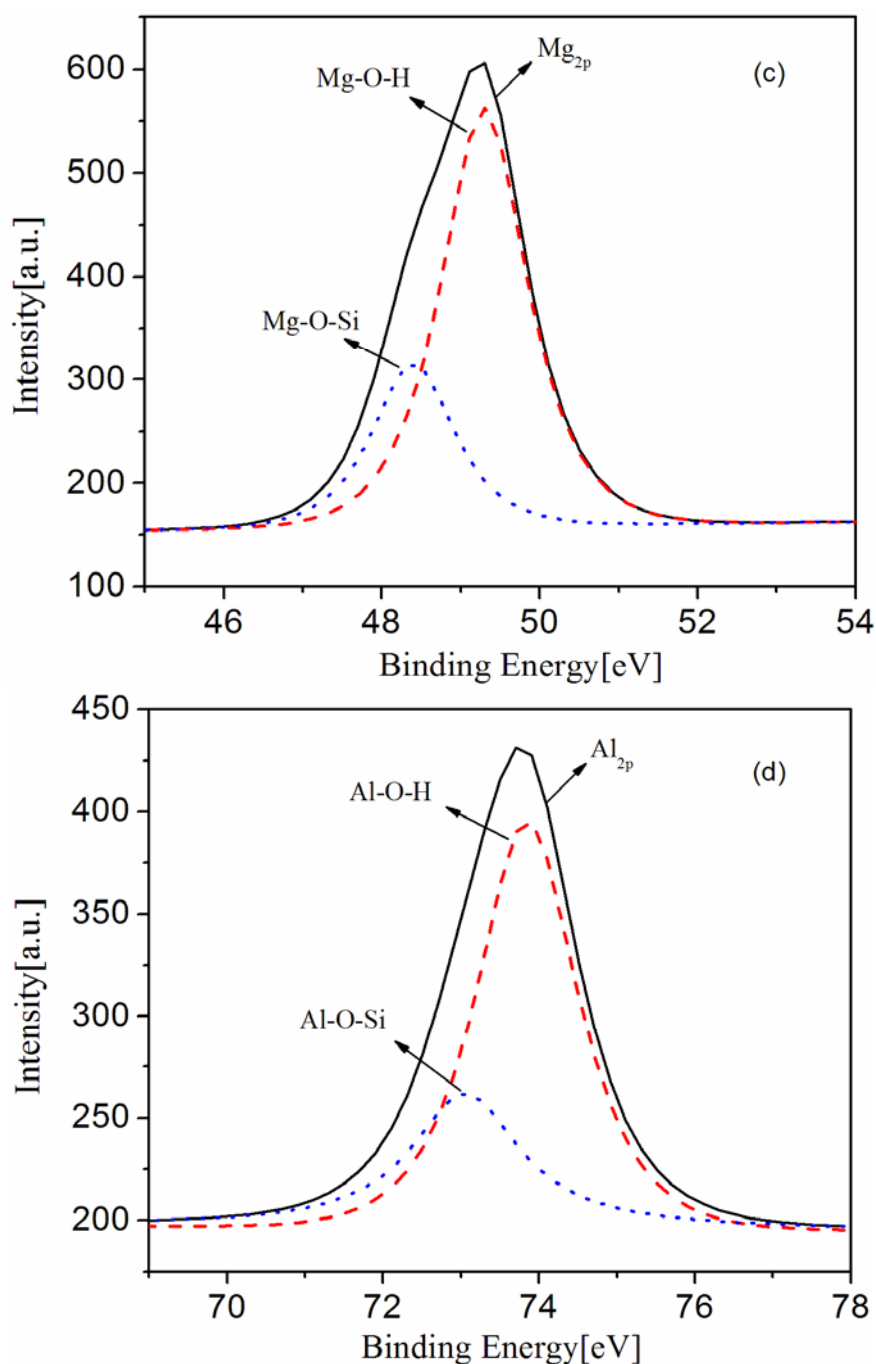
**Figure S3.** XPS spectra of the PEIE-HT complex: (a) C1s spectra; (b) Si2p spectra; (c) Mg2p spectra; (d) Al2p spectra.

## (3) TEM and STEM-EDS analysis

Figure S4(a) and Figure S4(b) are the TEM and STEM image of PEIE-HT complex, respectively. It can be seen that the reconstructed hydrotalcites are well dispersed in the polymer. And the C, O, N, Mg, Al and Si were detected by EDS. The STEM-EDS mapping (Figure S4 c-h) showed that Mg and Al were uniformly distributed in the C, O and N. Besides, the Si element showed a good match between other elements. The result indicated that this is a well dispersed system, and the PEIE and HT were coupled by the silane coupling agent(APTES).
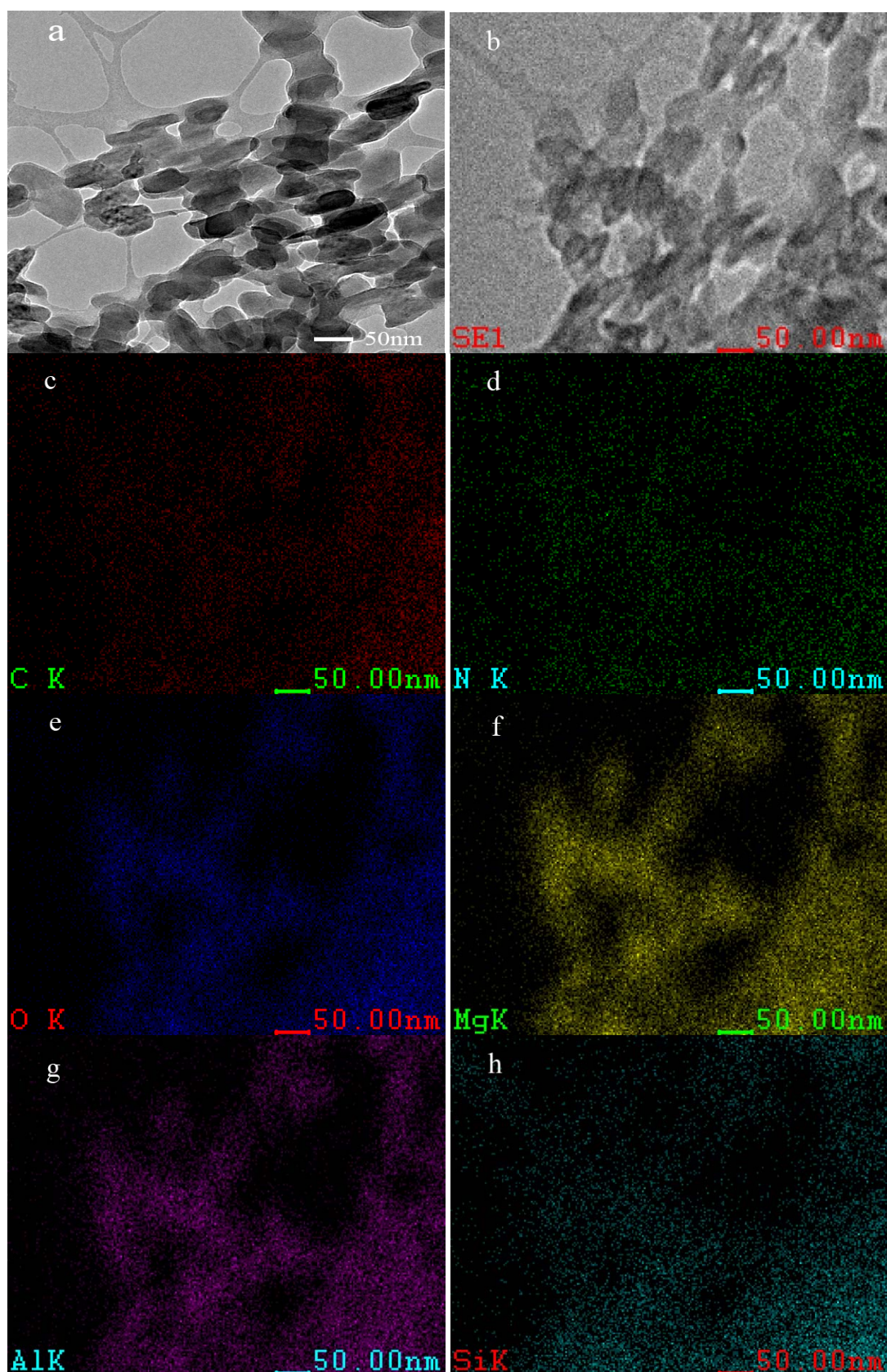
**Figure S4.** (a) TEM image of PEIE-HT complex; (b) STEM image of PEIE-HT complex; (c)-(h) STEM-EDS maps depict the distribution of the constituting elements, the images correspond to (c) the C K-edge, (d) the N K-edge and (e) the O K-edge, (f) the Mg K-edge and (g) the Al K-edge and (h) the Si K-edge signals, respectively.

## (4) XRD analysis

The characteristic peaks of hydrotalcite ($2\theta$=11.35°, 23.23°, 34.54°, 39.30°,46.82°,60.65° and 62.22°), corresponding to Miller indices (003), (006), (009), (015), (018), (110)and(113), were observed in Figure S5(a)[8, 41]. It demonstrate that the well-crystallized HT has been synthetised in this paper. After calcination, a series of peaks corresponding to HT are replaced by characteristic patterns of LDO ($2\theta$ =43.3° and 63.1°)[7], which were displayed in Figure S5(b). Moreover, the XRD patterns of PEIE presenced in a broad diffraction peak at $2\theta$=15-35° (Figure S5(c)). Compared with single substance, the XRD pattern of PEIE-HT complex contain the characteristic peaks of HT and the reflections of PEIE polymer, while the characteristic reflections of LDO at the $2\theta$ =43.3° and 63.1° were not appeared in the PEIE-HT complex. The results showed that the HT reconstructed successfully by using the LDO as raw material. It is worthwhile to note that the peaks of reconstructed HT in the PEIE is much lower than the peaks of the original HT (Figure S5(d)). This indicate that the superposition between layers of the reconstructed HT is reduces compared with the original HT. This also proved that the layer of the HT can be exfoliated and scattered by this method[42, 43]. Simultaneously, it is easy to find that the diffraction band ($2\theta$=15-35°) of PEIE in the complexes is lower than the peaks of original polymer at the corresponding location. This result indicates that the regular structure of polymer and HT was disrupted simultaneously by interpenetrating each other, and their crystallinity reduced.
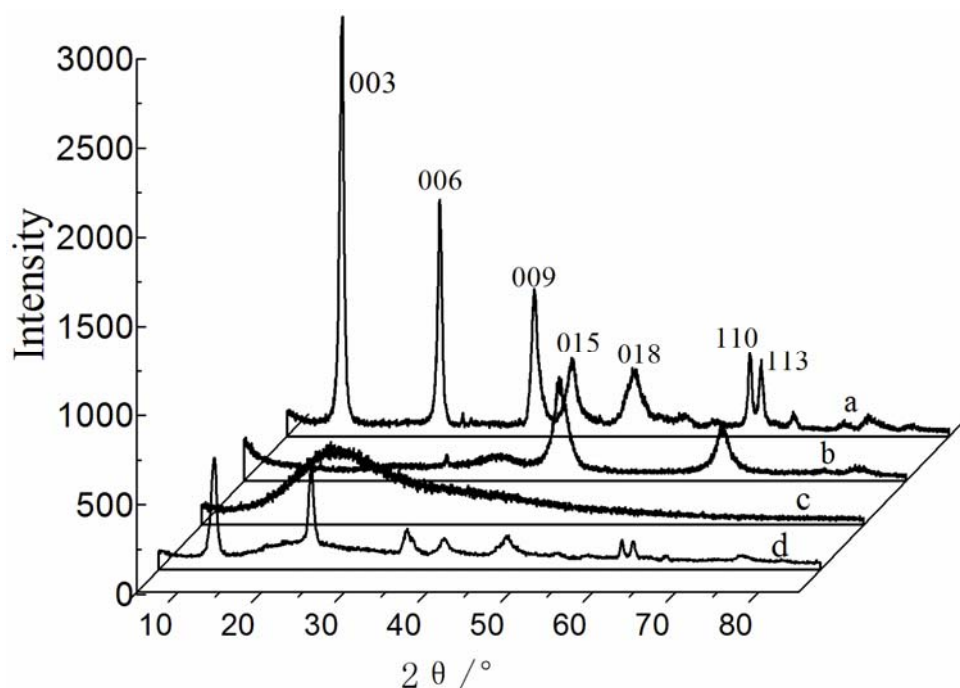


**Figure S5.** XRD patterns of (a) HT; (b) LDO; (c) PEIE; (d) PEIE-HT complex.
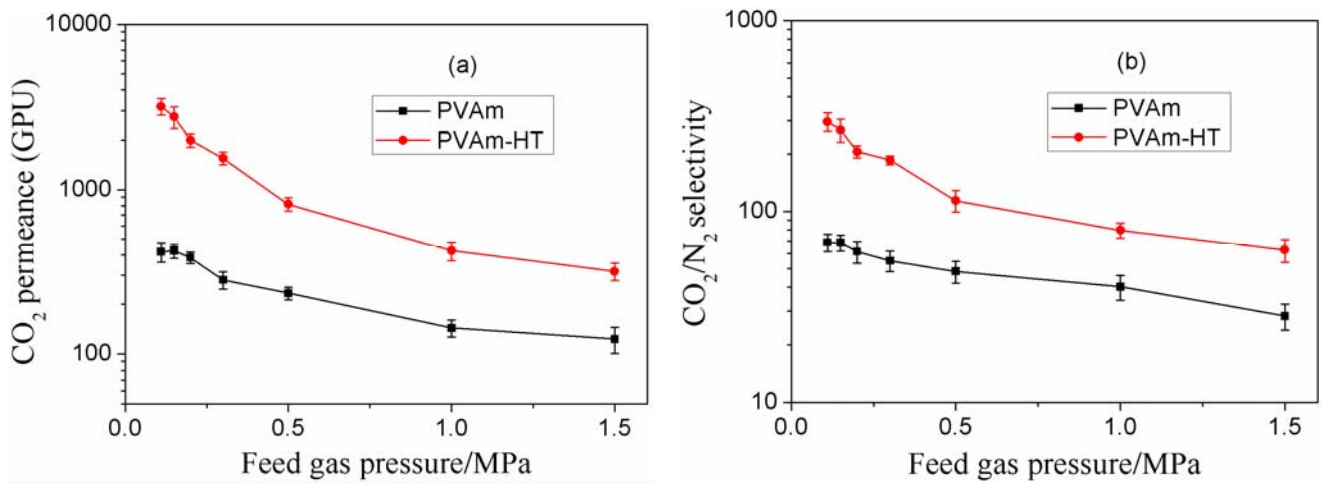
# 3 Performance comparison of membrane

**Table S2.** Performance comparison of the membrane obtained in this work
with other the state-of-the-art membranes

| NO. | Membrane | $R_{CO_2}$ (GPU) | $CO_2/N_2$ selectivity | Temperature (K) | Membrane type | Ref. |
|---|---|---|---|---|---|---|
| a | PEO-PBT(PAN-PMS) | 896 | 55 | 293 | CPM | [44] |
| b | Polaris[TM] | 1000 | 50 | 300.15 | CPM | [45] |
| c | Polaris[TM] | 2200 | 50 | 298.15 | CPM | [46] |
| d | Glycine-Na-Glycerol | 207 | 2090 | 296.15±2 | SLM | [47] |
| e | Glycine-Na | 648 | 5140 | 298.15 | SLM | [48] |
| f | PVBTAF | 11.3 | 983 | 296 | IEM | [49] |
| g | PE-AA- ethylenediamine | 100 | 4700 | — | IEM | [50] |
| h | PVAm/PVA | 212 | 174 | 298.15 | FCM | [51] |
| i | PVAm/PPO | 365 | 60 | 298.15 | FCM | [52] |
| j | DNMDAm-DGBAmE-TMC/PDMS | 1601 | 138 | 295.15 | FCM | [53] |
| k | (DAmBS–DGBAmE–TMC)/PDMS | 5831 | 86 | 298.15 | FCM | [54] |
| l | PVAm-PIP/PS | 6500 | 277 | 295.15 | FCM | [55] |
| m | PEIE-HT | 5693 | 268 | 298.15 | FCM | This work |

CPM: common polymeric membrane; SLM: supporting liquid membrane; IEM: ion-exchange membrane; FCM: fixed carrier
membrane;
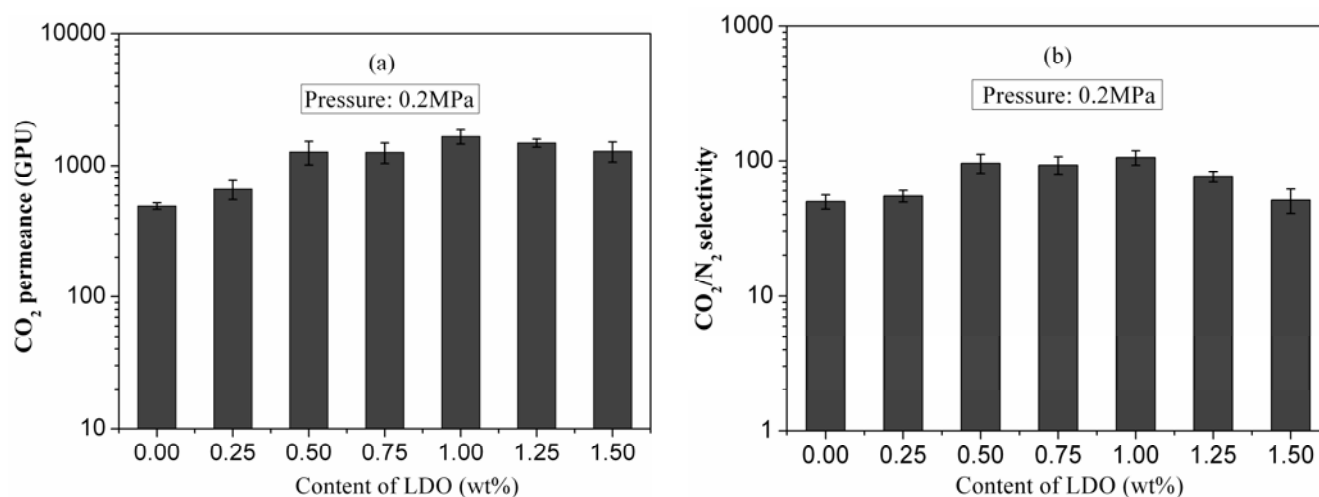


**Figure S6.** The effects of content of LDO (precursor of HT) on the performance of PEIE-HT membrane. Wet coating thickness: 50μm; Feed gas: 15vol% $CO_2$ and 85vol% $N_2$; 298.15K; Pressure: 0.2 Mpa.

**Figure S7.** Performance comparison of PVAm-HT membrane and PVAm membrane (a) $CO_2$ permeance; (b) $CO_2/N_2$ selectivity. Wet coating thickness: 50μm; Feed gas: 15vol% $CO_2$ and 85vol% $N_2$; 298.15K.
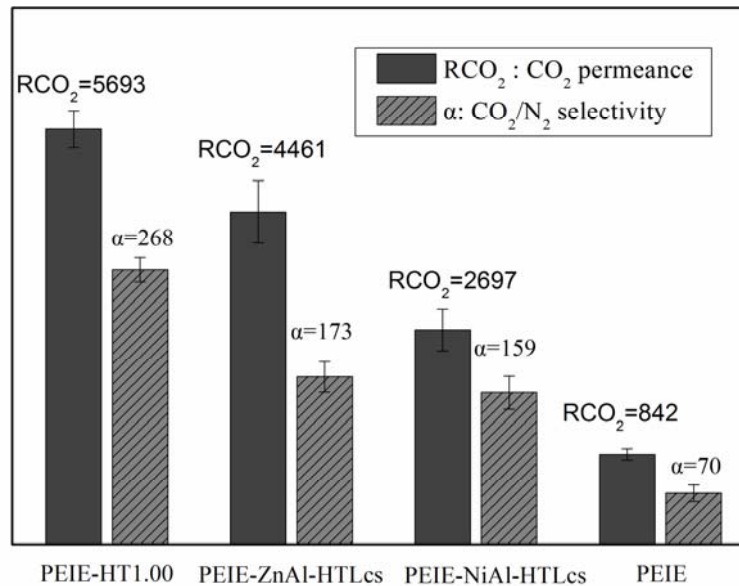


**Figure S8.** Performance comparison of the PEIE-HT membrane, PEIE-ZnAl- $CO_3^{2-}$-HTLcs membrane, PEIE-NiAl-$CO_3^{2-}$-HTLcs membrane and PEIE membrane. Wet coating thickness: 50μm; Feed gas: 15vol% $CO_2$ and 85vol% $N_2$; 298.15K; Pressure: 0.11 Mpa.

# 4 Stability of the PEIE-HT membrane in simulated flue gas



**Figure S9.** Separation performance stability at 0.11MPa and 1.5MPa. (a) Separation performance stability at 0.11MPa; (b) Separation performance stability at 1.5MPa. Wet coating thickness: 50μm; Feed gas: 15vol% $CO_2$ and 85vol% $N_2$; 298.15K.



**Figure S10.** The effects of temperature on the performance of PEIE-HT membrane. Wet coating thickness: 50μm; Feed gas: 15vol% $CO_2$ and 85vol% $N_2$; Pressure: 0.2 Mpa.



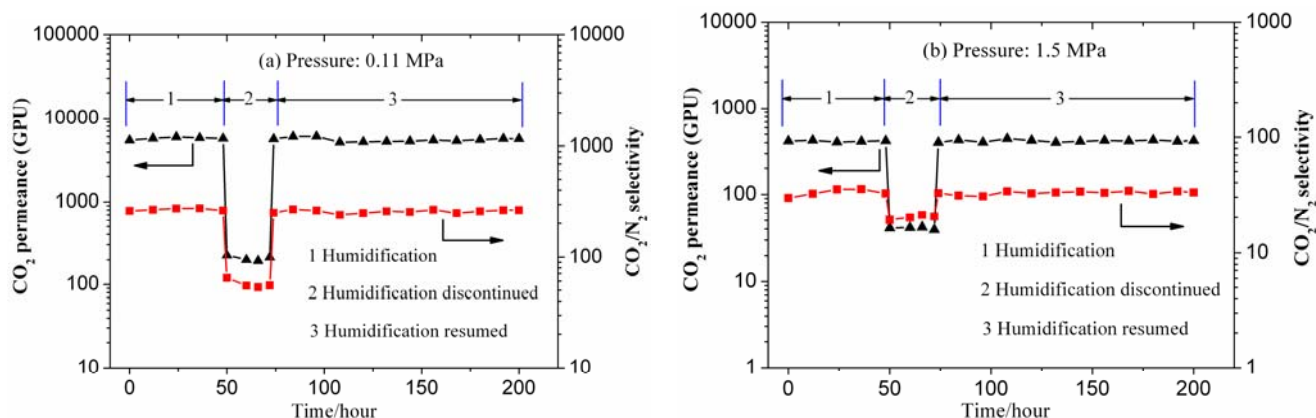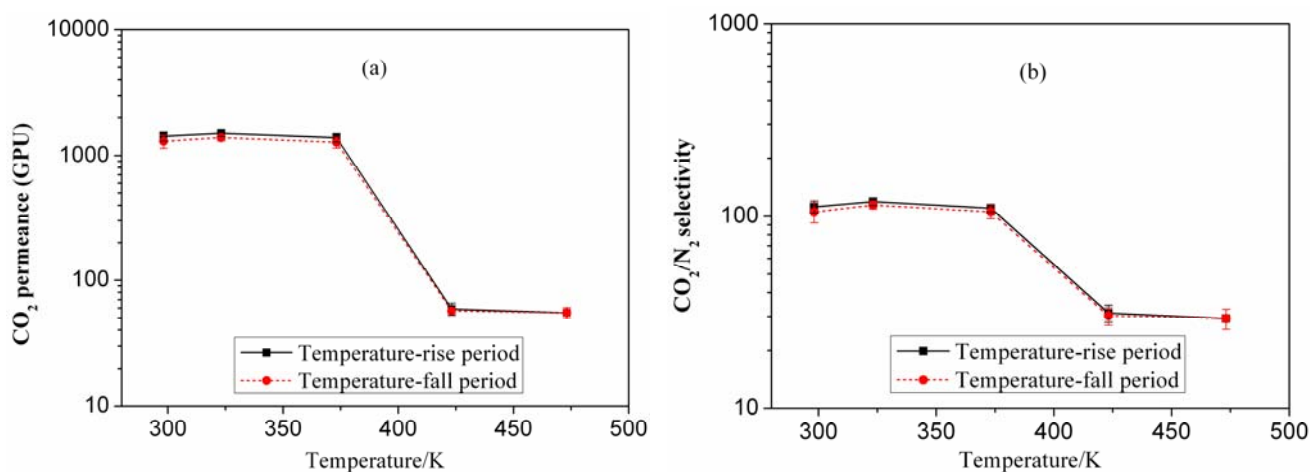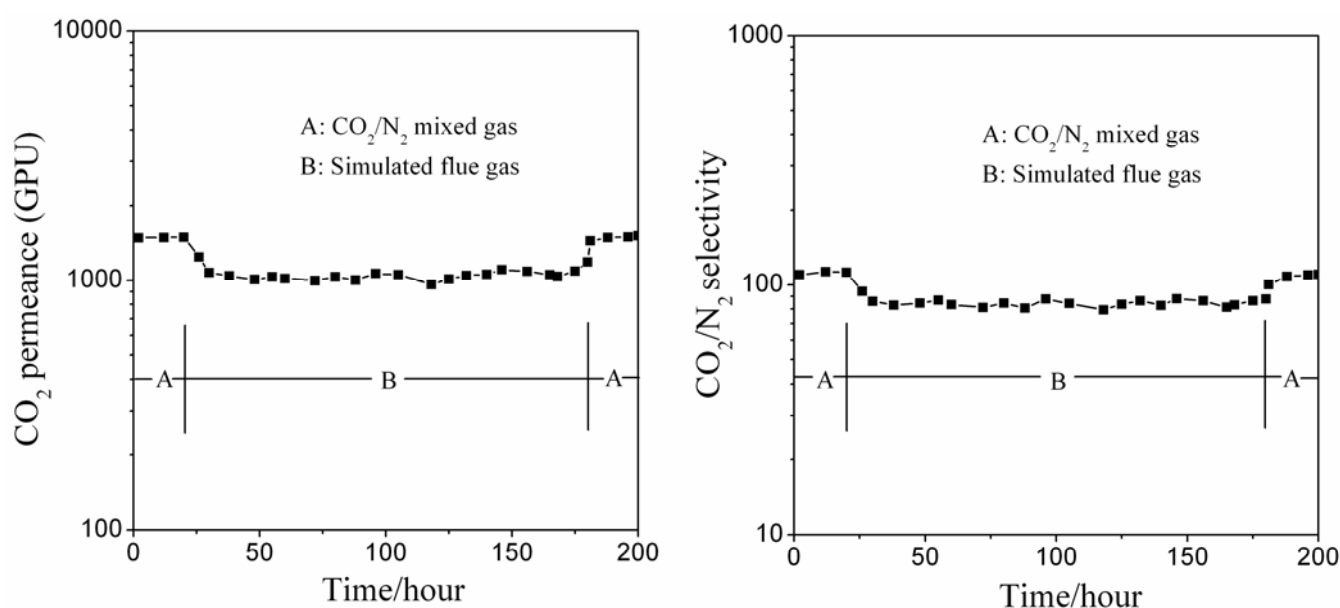**Figure S11.** PEIE-HT membrane tested by using $CO_2$/$N_2$ mixed gas (15vol% $CO_2$ and 85vol% $N_2$) and simulated flue gas(14.5vol% $CO_2$, 6.5vol% $O_2$, 40ppm $SO_2$, 70ppm $NO_2$, 10ppm CO, balanced by $N_2$). (a) $CO_2$ permeance; (b) $CO_2$/$N_2$ selectivity. Wet coating thickness: 50μm; 298.15K; Pressure: 0.2 MPa.
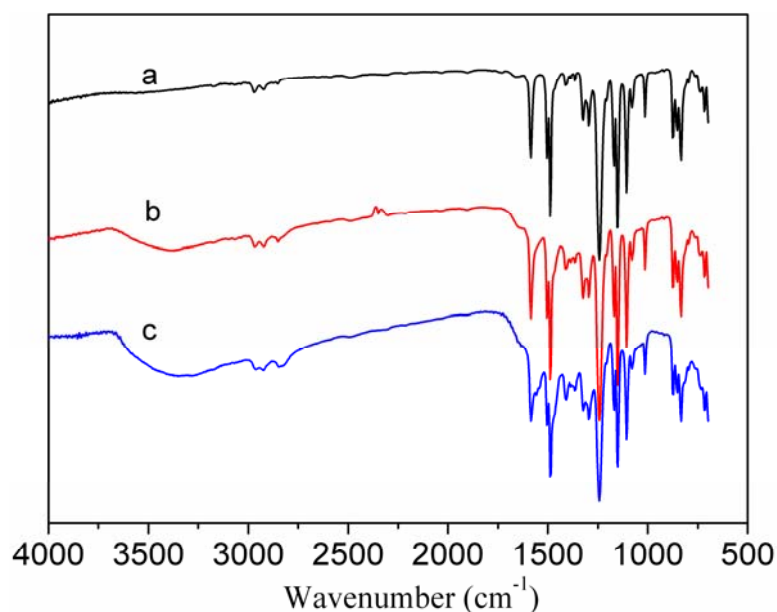
**Figure S12.** ATR-FTIR spectra of (a) polysulfone ultrafiltration membrane; (b) original PEIE-HT membrane ; (c) PEIE-HT membrane after being tested in simulated flue gas.

**Table S3 (a)**. The surface elemental analysis for original PEIE-HT membrane.

| Element | C1s | N1s | O1s | Mg2p | Al2p | Si2p | S2p |
|---|---|---|---|---|---|---|---|
| Relative atomic ratio (atm.%) | 48.85 | 13.59 | 26.73 | 6.86 | 2.81 | 1.03 | 0.13 |
| Binding energy(eV) | 284.80 | 398.36 | 531.08 | 49.45 | 73.73 | 101.27 | 168.21 |

**Table S3 (b)**. The surface elemental analysis for PEIE-HT membrane after being tested in simulated flue gas.

| Element | C1s | N1s | O1s | Mg2p | Al2p | Si2p | S2p |
|---|---|---|---|---|---|---|---|
| Relative atomic ratio (atm.%) | 49.17 | 15.31 | 24.27 | 7.56 | 2.61 | 0.92 | 0.16 |
| Binding energy(eV) | 284.80 | 398.36 | 530.89 | 49.21 | 73.69 | 101.62 | 168.02 |

## 5 Experimental

**Synthesis of PEIE:** Polyethyleinimine and epichlorohydrin copolymer (PEIE) was synthesized via block polymerization. In a 100ml round bottom flask equipped with a mechanical agitator, a constant pressure dropping funnel and a reflux condenser, 20g 10% PEI was charged. Under the protection of nitrogen, 0.14g epichlorohydrin was dropped into the flask with 4~6 drops/min at 308.15K controlled by water bath while stirring. After dropping, keep at 308.15K for 1h and then heat to 328.15K for 24h. Then, a certain amount of deionized water was added and a colorless, transparent viscous solution was obtained. The polymer solution was mixed with anion exchange resin(Amberlite 717) and was further stirred for 2h. Finally, the PEIE aqueous solution was obtained by vacuum filtration of the mixture.

**Synthesis of HT and LDO:** The synthesis of HT was carried out in a three-neck flask equipped with a reflux condenser. In a typical procedure, 0.09mol $Mg(NO_3)_2·6H_2O$ and 0.03mol $Al(NO_3)_3·9H_2O$ were dissolved in 100ml mixed solution ($H_2O$/ethanol=80/20, by volume) . Then, the mixed basic solution(contain 2M NaOH and 1M $Na_2CO_3$) was dropped into the flask with stirring until the pH value equal to 10. The slurry thus obtained was stirred for an additional 30 min, and then was put into a stainless steel reactor, and was hydrothermally treated at 393.15K for 24h. The resulting white, solid product was filtered, washed with deionized water and absolute ethanol several times, and finally dried under vacuum at 353.17K for 24h. The LDO was obtained by calcined HT in air atmosphere at 673.15K for 5h.

**Preparation of PEIE-HT complex and PEIE-HT membrane:** 1.0wt% LDO was mixed in 1.5wt% PEIE solution with intensely stirring to distribute the particles uniformly. It was stirring continually for 5 day to reconstruct HT, afterwards 0.1wt% APTES was added and reacted at 353.15K for 2h and the PEIE-HT complex was obtained. The PEIE-HT membrane was prepared by casting the PEIE-HT complex solution on porous polysulfone ultrafiltration membrane under 303.15K and 40% relative humidity, and then dried at the same condition over night.

**Gas permeation measurements:** The gas permselectivity of membranes was characterized at 298.15K by a homemade apparatus with humidifier detailed in literature[54]. The membrane was mounted in a circular stainless steel cell (effective membrane area=19.26cm$^2$). Both the feed gas and the sweep gas ($H_2$) were saturated with water. The flow of outlet sweep gas was measured using a soap film meter and its composition was analyzed by a gas chromatograph  equipped with athermal conductivity detector (HP7890, Porapak N). It has been proved that the effect of both back-diffusion of $H_2$ and concentration polarization on data analysis could be neglected[54, 55].

# 6  Characterization techniques in the experiment

To characterize the structure of PEIE-HT complex, the PEIE-HT complex solution was coated on the polytetrafluoroethene substrate, then drying at 303.15K and 40% relative humidity in an artificial climate chamber (Climacell 222R, Germany) for 24 hours, finally, the PEIE-HT complex film was peeled from the polytetrafluoroethene substrate. This film was used as the test sample of TG-MS, $N_2$ adsorption-desorption ATR-FTIR, XPS, and XRD. And the PEIE-HT complex solution was used to fabricate TEM, STEM-EDS sample.

The TG of each sample and the MS profile of the evolved gaseous water (m/z =18) and carbon dioxide (m/z =44) were collected by means of NETZSCH Simultaneous TG-DTA/DSC (Apparatus STA 449C/4/G Jupiter-QMS 403C Aeolos) in $N_2$ atmosphere at a ramping rate of 2K/min from 300.15K to 973.15 K. For each measurement, about 50-60 mg of dried sample was used. The $N_2$ adsorption-desorption experiments were measured with a Micromeritics ASAP 2010 automatic analyzer.

Attenuated total reflectance infrared (ATR-FTIR) spectroscopy (FTS-6000, Bio-Rad of USA) was used to study the chemical structure of sample. The chemical characterization of sample was further accomplished by X-ray photoelectron spectroscopy (XPS, PHI-1600). XPS analysis was performed using Mg Kα as the radiation source and the spectra were taken with the electron emission angle at 45º. X-ray diffraction (XRD) patterns were recorded on Rigaku D/max-2500 (40 kV, 100 mA) using Cu Kα radiation at a scanning rate of 2θ = 10º /min, in the scanning range of 5º −85º.

Both TEM and STEM studies were performed using a JEOL JEM-2100F field emission transmission electron microscope equipped with an ultra high resolution pole-piece operating at 200 kV. Energy dispersive X-ray spectrometer (EDS) attached to the JEM-2100F microscope was used to determine the elemental composition of the samples. TEM specimens were prepared by placing microdrops of PEIE-HT complex solution directly onto a copper grid coated with carbon film (300 mesh, EMS).

Scanning electron microscopy (SEM) images of the surface and the cross-section for the PEIE-HT/PS composite membranes were obtained on Nova NanoSEM 430 (FEI, USA). For the cross-section observation, the membrane samples were prepared by peeling away the polyester backing fabric, then frozen in liquid nitrogen and fractured. All membrane samples were coated with gold by a sputter-coating machine.

# References

1. H. A. Prescott, Z.-J. Li, E. Kemnitz, A. Trunschke, J. Deutsch, H. Lieske and A. Auroux, *J. Catal.*, 2005, **234**, 119-130.
2. K. Teramura, S. Iguchi, Y. Mizuno, T. Shishido and T. Tanaka, *Angew. Chem.*, 2012, **124**, 8132-8135.
3. J. Zhang, Y. F. Xu, G. Qian, Z. P. Xu, C. Chen and Q. Liu, *J. Phys. Chem. C*, 2010, **114**, 10768-10774.
4. B. M. Choudary, M. L. Kantam, A. Rahman, C. V. Reddy and K. K. Rao, *Angew. Chem.*, 2001, **113**, 785-788.
5. H. Fei, M. R. Bresler and S. R. J. Oliver, *J. Am. Chem. Soc.*, 2011, **133**, 11110-11113.
6. P. J. Sideris, U. G. Nielsen, Z. Gan and C. P. Grey, *Science*, 2008, **321**, 113-117.
7. F. Millange, R. I. Walton and D. O'Hare, *J. Mater.Chem.*, 2000, **10**, 1713-1720.
8. M. Ogawa and H. Kaiho, *Langmuir*, 2002, **18**, 4240-4242.
9. T. R. Boussie, G. M. Diamond, C. Goh, K. A. Hall, A. M. LaPointe, M. K. Leclerc, V. Murphy, J. A. W. Shoemaker, H. Turner, R. K. Rosen, J. C. Stevens, F. Alfano, V. Busico, R. Cipullo and G. Talarico, *Angew. Chem. Int.Ed.*, 2006, **45**, 3278-3283.
10. S. Suganuma, K. Nakajima, M. Kitano, D. Yamaguchi, H. Kato, S. Hayashi and M. Hara, *J. Am. Chem. Soc.*, 2008, **130**, 12787-12793.
11. Y. Zhong, F. Peng, X. Wei, Y. Zhou, J. Wang, X. Jiang, Y. Su, S. Su, S.-T. Lee and Y. He, *Angew. Chem. Int. Ed.*, 2012, **51**, 8485-8489.
12. M. de Loos, J. van Esch, R. M. Kellogg and B. L. Feringa, *Angew. Chem.*, 2001, **113**, 633-636.
13. B. M. Choudary, M. L. Kantam, A. Rahman, C. V. Reddy and K. K. Rao, *Angew. Chem. Int. Ed.*, 2001, **40**, 763-766.
14. A. Corma, P. Concepción and P. Serna, *Angew. Chem.*, 2007, **119**, 7404-7407.
15. N. A. Dhas, A. Zaban and A. Gedanken, *Chem. Mater.*, 1999, **11**, 806-813.

16.     Ö. Çelik and Ö. Dag, *Angew. Chem.* 2001, **113**, 3915-3919.

17.     E. Finocchio, G. Garuti, M. Baldi and G. Busca, *Chemosphere*, 2008, **72**, 1659-1663.

18.     N. Hering, K. Schreiber, R. Riedel, O. Lichtenberger and J. Woltersdorf, *Appl. Organomet. Chem.*, 2001, **15**, 879-886.

19.     J. Jeong, M. Cho, Y. T. Lim, N. W. Song and B. H. Chung, *Angew. Chem. Int. Ed.*, 2009, **48**, 5296-5299.

20.     A. J. Patil, E. Muthusamy, A. M. Seddon and S. Mann, *Adv. Mater.*, 2003, **15**, 1816-1819.

21.     T. Sugama, R. Sabatini and L. Petrakis, *Ind. Eng. Chem. Res.*, 1998, **37**, 79-88.

22.     F. Wypych, W. H. Schreiner, N. Mattoso, D. H. Mosca, R. Marangoni and C. A. da S. Bento, *J. Mater. Chem.*, 2003, **13**, 304-307.

23.     T. Cha, A. Guo, Y. Jun, D. Pei and X.-Y. Zhu, *PROTEOMICS*, 2004, **4**, 2823-2823.

24.     G. G. Condorelli, A. Motta, M. Favazza, I. L. Fragalà, M. Busi, E. Menozzi, E. Dalcanale and L. Cristofolini, *Langmuir*, 2006, **22**, 11126-11133.

25.     H. J. Martin, K. H. Schulz, J. D. Bumgardner and K. B. Walters, *Langmuir*, 2007, **23**, 6645-6651.

26.     Z. Qian, Z. Zhang, L. Song and H. Liu, *J. Mater. Chem.*, 2009, **19**, 1297-1304.

27.     M.-R. Choi, T.-H. Han, K.-G. Lim, S.-H. Woo, D. H. Huh and T.-W. Lee, *Angew. Chem.*, 2011, **123**, 6398-6401.

28.     L. Li and H. Yokoyama, *Angew. Chem.*, 2006, **118**, 6486-6489.

29.     H. Nakano, T. Mitsuoka, M. Harada, K. Horibuchi, H. Nozaki, N. Takahashi, T. Nonaka, Y. Seno and H. Nakamura, *Angew. Chem. Int. Ed.*, 2006, **45**, 6303-6306.

30.     Y. Vaynzof, T. J. K. Brenner, D. Kabra, H. Sirringhaus and R. H. Friend, *Adv. Funct. Mater.*, 2012, **22**, 2418-2424.

31.     B. D. Freeman, *NOVEL NANOCOMPOSITE MEMBRANE STRUCTURES FOR H2 SEPARATIONS*, 2005.

32.     N. Maxim, P. C. M. M. Magusin, P. J. Kooyman, J. H. M. C. van Wolput, R. A. van Santen and H. C. L. Abbenhuis, *Chem. Mater.*, 2001, **13**, 2958-2964.

33.     H. Nakayama and T. Hata, *Thin Solid Films*, 2006, **501**, 190-194.

34.     F. Thieblemont, O. Seitz, A. Vilan, H. Cohen, E. Salomon, A. Kahn and D. Cahen, *Adv. Mater.*, 2008, **20**, 3931-3936.

35.     R. Voicu, R. Boukherroub, V. Bartzoka, T. Ward, J. T. C. Wojtyk and D. D. M. Wayner, *Langmuir*, 2004, **20**, 11713-11720.

36.     Y. Yang, G. Meng, X. Liu and L. Zhang, *Angew. Chem.*, 2008, **120**, 371-373.

37.     H. Y. Kim, H. M. Lee and J.-N. Park, *J. Phys. Chem. C*, 2010, **114**, 7128-7131.

38.     L. Ukrainczyk, R. A. Bellman and A. B. Anderson, *J. Phys. Chem. B*, 1997, **101**, 531-539.

39.     J. A. Boscoboinik, X. Yu, B. Yang, F. D. Fischer, R. Włodarczyk, M. Sierka, S. Shaikhutdinov, J. Sauer and H.-J. Freund, *Angew. Chem. Int. Ed.*, 2012, **51**, 6005-6008.

40.     X. Zhang, G. Zhuang, J. Chen, Y. Wang, X. Wang, Z. An and P. Zhang, *J. Phys. Chem. B*, 2006, **110**, 12588-12596.

41.     R. k. Allada, A. Navrotsky, H. T. Berbeco and W. H. Casey, *Science*, 2002, **296**, 721-723.

42.     G. S. Attard, J. M. Corker, C. G. Göltner, S. Henke and R. H. Templer, *Angew. Chem. Int. Ed. in English*, 1997, **36**, 1315-1317.

43.     E. Kockrick, P. Krawiec, W. Schnelle, D. Geiger, F. M. Schappacher, R. Pöttgen and S. Kaskel, *Adv. Mater.*, 2007, **19**, 3021-3026.

44.     Y. Wilfredo, C. Anja, W. Jan and P. Klaus-Viktor, *Nanotechnology*, 2010, **21**, 395301.

45.     T. C. Merkel, H. Lin, X. Wei and R. Baker, *J. Membr. Sci.*, 2010, **359**, 126-139.

46.     T. C. Merkel, X. Wei, Z. He, L. S. White, J. G. Wijmans and R. W. Baker, *Ind. Eng. Chem. Res.*, 2012, **52**, 1150-1159.

47.     H. Chen, A. S. Kovvali and K. K. Sirkar, *Ind. Eng. Chem.Res.*, 2000, **39**, 2447-2458.

48.     H. C. A. S. Kovvali, G. Obuskovic, S. Majumdar, A. K. Sirkar, *Abs. Pap. Am. Chem. Soc.*, 2000, **220**, U392-U392.

49.     R. Quinn and D. V. Laciak, *J. Membr. Sci.*, 1997, **131**, 49-60.

50.  H. Matsuyama, M. Teramoto and K. Iwai, *J. Membr. Sci.*, 1994, **93**, 237-244.

51.  L. Deng, T.-J. Kim and M.-B. Hägg, *J. Membr. Sci.*, 2009, **340**, 154-163.

52.  M. Sandru, S. H. Haukebø and M.-B. Hägg, *J. Membr. Sci.*, 2010, **346**, 172-186.

53.  S. Li, Z. Wang, X. Yu, J. Wang and S. Wang, *Adv. Mater.*, 2012, **24**, 3196-3200.

54.  M. Wang, Z. Wang, S. Li, C. Zhang, J. Wang and S. Wang, *Energy Environ.l Sci.*, 2013.

55.  Z. Qiao, Z. Wang, C. Zhang, S. Yuan, Y. Zhu, J. Wang and S. Wang, *AIChE J.*, 2013, **59**, 215-228.